Receptor-mediated and bulk-phase endocytosis cause macrophage and cholesterol accumulation in Niemann-Pick C disease

Benny Liu,* Chonglun Xie,* James A. Richardson,† Stephen D. Turley,* and John M. Dietschy[1,*]

Departments of Internal Medicine* and Pathology,† University of Texas Southwestern Medical School, Dallas, TX 75390-9151

Abstract **These studies explored the roles of receptor-mediated and bulk-phase endocytosis as well as macrophage infiltration in the accumulation of cholesterol in the mouse with Niemann-Pick type C (NPC) disease. Uptake of LDL-cholesterol varied from 514 μg/day in the liver to zero in the central nervous system. In animals lacking LDL receptors, liver uptake remained about the same (411 μg/day), but more cholesterol was taken up in extrahepatic organs. This uptake was unaffected by the reductive methylation of LDL and consistent with bulk-phase endocytosis. All tissues accumulated cholesterol in mice lacking NPC1 function, but this accumulation was decreased in adrenal, unchanged in liver, and increased in organs like spleen and lung when LDL receptor function was also deleted. Over 56 days, the spleen and lung accumulated amounts of cholesterol greater than predicted, and these organs were heavily infiltrated with macrophages. This accumulation of both cholesterol and macrophages was increased by deleting LDL receptor function. These observations indicate that both receptor-mediated and bulk-phase endocytosis of lipoproteins, as well as macrophage infiltration, contribute to the cholesterol accumulation seen in NPC disease. These macrophages may also play a role in parenchymal cell death in this syndrome.**—Liu, B., C. Xie, J. A. Richardson, S. D. Turley, and J. M. Dietschy. **Receptor-mediated and bulk-phase endocytosis cause macrophage and cholesterol accumulation in Niemann-Pick C disease.** ***J. Lipid Res.*** **2007.** 48: **1710–1723.**

Supplementary key words hepatic dysfunction • lung failure • low density lipoprotein receptor • lysosomal cholesterol • apoptosis • neurodegeneration • lipoprotein clearance

Receptor-mediated endocytosis of lipoproteins through clathrin-coated pits plays a major role in the cellular uptake of cholesterol from the plasma. Although the general outline of this clathrin-coated pit pathway is understood, there are several major quantitative details that are still poorly defined but that may be important in understanding the pathophysiology of such diverse diseases as familial hypercholesterolemia and Niemann-Pick type C (NPC) disease. The major lipoproteins in the plasma expressing apolipoprotein E (apoE) are chylomicron remnants (CMrs) and very low density lipoprotein remnants (VLDLrs), whereas the major fraction expressing apoB-100 is LDL (1, 2). As illustrated in **Fig. 1**, to reach the surface of the parenchymal cell, these lipoproteins must traverse the barrier represented by the endothelial lining of the capillaries. Some of these capillaries, like those in the central nervous system, are impermeable to these particles (3, 4). Other capillaries, like those in the liver, have large fenestrations of 50–90 nm in diameter that are freely permeable to lipoproteins (5).

These apoE- and apoB-100-containing particles that reach the pericellular space compete for binding to low density lipoprotein receptors (LDLRs) on the plasma membrane of the various cells (Fig. 1, step A) (6, 7). These ligand/receptor complexes then concentrate and cluster into coated pits (step B) and, along with a small volume of bulk pericellular fluid, are endocytosed into the cell (step C). A vacuolar ATPase translocates protons into these vesicles, acidifying the contents of the endosome (step D), which leads to unfolding of the LDLR, release of the lipoprotein particle, and hydrolysis of the cholesteryl ester by lysosomal acid lipase (8). The unesterified cholesterol formed by this reaction in the late endosomal/lysosomal compartment (step E) is solubilized by NPC2 protein (9, 10) and then transported into the cytosol by NPC1 protein (step F) (11–14). This cholesterol, along with newly synthesized sterol (step H), forms a metabolically available pool of cholesterol (step G) that is used for a variety of purposes by the cell. The size of this metabolically active pool is sensed and tightly regulated by mechanisms in the endoplasmic reticulum and nucleus that can alter the level of LDLR activity in the cell mem-

Manuscript received 13 March 2007 and in revised form 19 April 2007.

Published, JLR Papers in Press, May 2, 2007.
DOI 10.1194/jlr.M700125-JLR200

Abbreviations: apoE, apolipoprotein E; CMr, chylomicron remnant; LDL-TC, total cholesterol carried in LDL; LDLR, low density lipoprotein receptor; NPC, Niemann-Pick type C; VLDLr, very low density lipoprotein remnant.

[1] To whom correspondence should be addressed.
e-mail: john.dietschy@utsouthwestern.edu

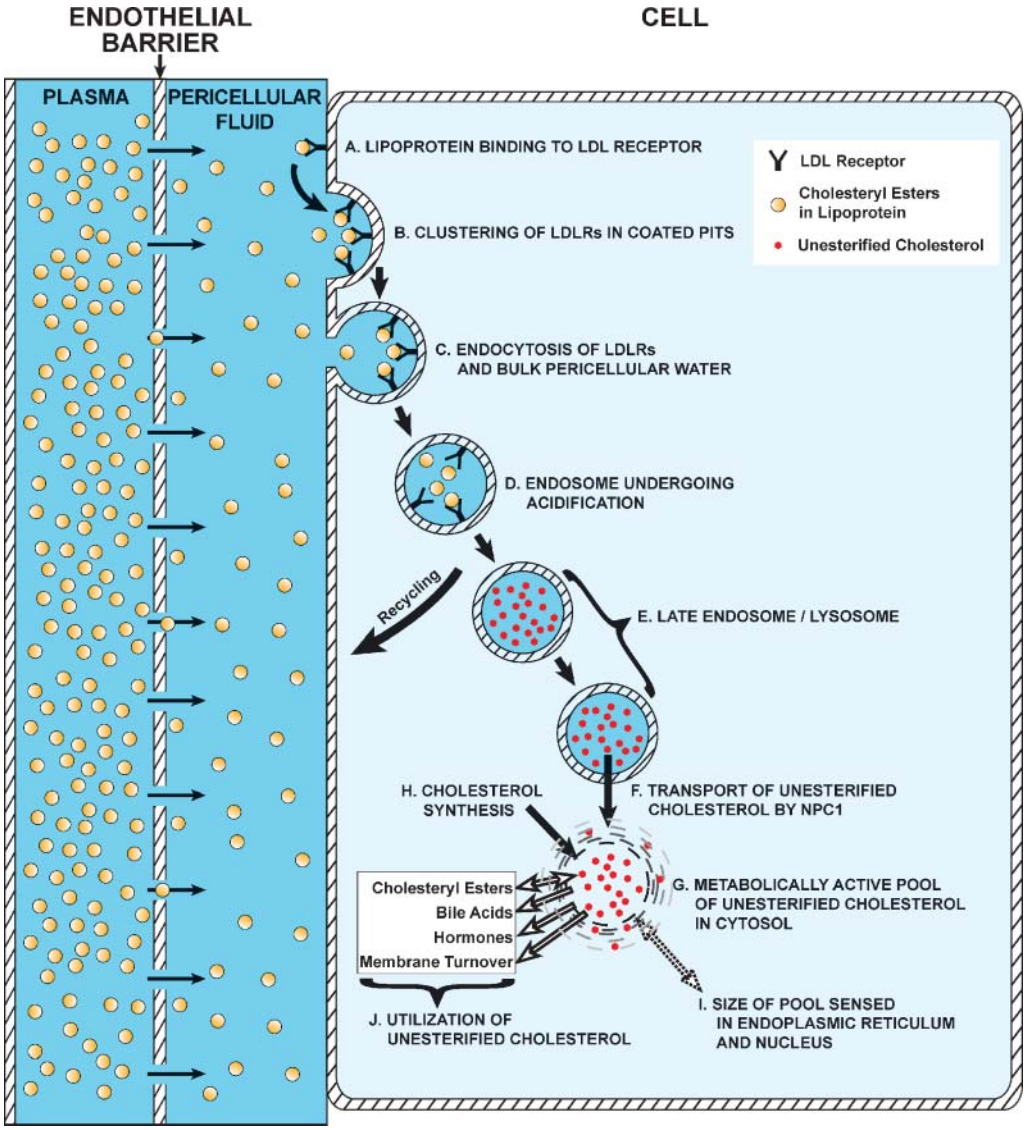

Fig. 1. Diagrammatic representation of the processes of receptor-mediated and bulk-phase endocytosis of lipoprotein particles into the cells of the body. Plasma lipoproteins such as LDL carrying predominantly cholesteryl ester must diffuse from the plasma space across the endothelial barrier into the pericellular fluid. The resistance of this endothelial barrier to diffusion of the lipoprotein particles can be described by a reflection coefficient in which a value of 0 represents no resistance and a value of 1.0 represents infinite resistance. The lipoprotein particles may then enter the endocytic vesicle of a clathrin-coated pit after binding to an LDL receptor (steps A, B) or in solution in the pericellular bulk solution (step C). After various steps, designated D–G, the unesterified cholesterol that is formed is transported from the late endosomal/lysosomal compartment into a metabolically accessible pool of sterol in the cytosolic compartment. The net transport of the lipoprotein particles, therefore, takes place by two independent processes that are either receptor-dependent or receptor-independent, bulk-phase uptake. In both cases, the lipoproteins are fed into the late endosomal/lysosomal compartment for processing. NPC1, Niemann-Pick type C1.

brane, the rate of sterol synthesis, and the rate of sterol export (15, 16). In this manner, the absolute concentration of cholesterol in every cell is kept remarkably constant over the life of an animal or human, and the various apoE- and apoB-100-containing lipoproteins are efficiently removed from the plasma.

This whole system, however, breaks down in the face of mutations that inactivate one of the proteins mediating the three major steps in this sequence. Mutations of the LDLR (familial hypercholesterolemia), for example, lead to marked increases of the plasma cholesterol concentration but essentially no detectable change in the cellular level of sterol or the rate of cholesterol synthesis (17, 18). In contrast, a mutation in lysosomal acid lipase (Wolman disease) causes a major increase in the contents of cholesteryl ester and triacylglycerol, presumably in the late endosomal/lysosomal compartment, in the cells of many organs, yet the plasma cholesterol concentration remains

relatively unchanged (19, 20). Similarly, mutations inactivating NPC1 or NPC2 (NPC disease) lead to massive accumulation of unesterified cholesterol, but not triacylglycerol, in the late endosomal/lysosomal compartment of the cells in all tissues but only a marginal increase of the circulating cholesterol concentration in the plasma (21).

These observations highlight a number of uncertainties concerning this whole pathway of receptor-mediated endocytosis. If, for example, the LDLR is responsible for the uptake of lipoproteins such as LDL, what process accounts for the clearance of these particles when the LDLR is nonfunctional, and why is there little evidence of altered cellular cholesterol homeostasis in this syndrome? Furthermore, what characteristics of this putative second transport process could account for the fact that it clears more cholesterol associated with LDL (LDL-TC) from the plasma each day than normally is cleared when the LDLR is functional (22)? Additionally, if the accumulation of unesterified cholesterol in cells with mutational inactivation of NPC1 comes from lipoprotein sterol bound to the LDLR, why doesn't deletion of the function of this receptor markedly decrease the rate of sterol accumulation in the NPC syndrome? Such a manipulation actually decreases the cholesterol content in a few tissues but increases it in most others (23, 24). Finally, is there a different role in monocytes and macrophages for lipoprotein clearance through receptor-mediated endocytosis or other mechanisms in NPC disease?

To explore these questions and further understand the pathogenesis of NPC disease, the current studies examined five specific areas of lipoprotein transport. The first set of experiments quantitated the rates of clearance of LDL-TC in mice, both in the presence and absence of the LDLR. A second group of studies explored whether there was residual LDLR binding activity in animals supposedly lacking LDLRs. A third set of experiments measured the rates of bulk-phase endocytosis and determined whether this process, as well as receptor-mediated uptake, delivered cholesterol into the late endosomal/lysosomal compartment. A fourth group of experiments compared actual rates of cholesterol accumulation in the tissues of animals lacking NPC1 function with the theoretical rates of lipoprotein cholesterol uptake by both receptor-mediated and bulk-phase endocytosis. Finally, a histological survey of the various organs in these animals was undertaken to determine whether there were significant differences in macrophage recruitment and cholesterol accumulation in mice lacking functional NPC1 activity compared with those lacking functional LDLR activity.

MATERIALS AND METHODS

Animals and diets

These studies were undertaken using three different groups of genetically modified mice in addition to appropriate control animals (designated $ldlr^{+/+}/npc1^{+/+}$). These groups included animals lacking LDLR activity ($ldlr^{-/-}/npc1^{+/+}$), mice lacking functional NPC1 activity ($ldlr^{+/+}/npc1^{-/-}$), and animals lacking the activity of both of these proteins ($ldlr^{-/-}/npc1^{-/-}$) (17, 21, 25). These animals were housed in plastic colony cages in rooms with alternating 12 h periods of light and dark. All animals were fed ad libitum a low-cholesterol (0.02%, w/w) rodent pellet diet (No. 7001; Harlan Teklad, Madison, WI) until they were studied at ~7–9 weeks of age. All experiments were carried out during the fed state, ~1–2 h before the end of the dark cycle, and the experimental groups contained equal numbers of male and female animals. All experimental protocols were approved by the Institutional Animal Care and Use Committee of the University of Texas Southwestern Medical Center.

Isolation and radiolabeling of LDL and albumin

Mouse LDL was harvested from both male and female $ldlr^{-/-}$ mice that had been maintained on a low-cholesterol diet, whereas ovine and human LDL was obtained from the plasma of normocholesterolemic sheep and humans, respectively. In all cases, the LDL fraction was isolated by preparative ultracentrifugation in the density range of 1.020–1.055 g/ml. These LDL preparations, along with mouse albumin (Sigma, St. Louis, MO), were then radiolabeled with either [^{125}I]tyramine cellobiose or ^{131}I (17, 23, 26, 27). The apoE-containing HDL contaminating some of these LDL fractions was removed by passing the lipoprotein solution over a heparin-Sepharose 6b column (28). In one case, a portion of the human LDL was reductively methylated to block its interaction with the LDLR (29). After extensive dialysis, these radiolabeled preparations were passed through a 0.45 μm Millex-HA filter.

Measurement of clearance rates for LDL and albumin

Mice were anesthetized and a catheter was inserted into a jugular vein. After awakening, each animal was given a bolus of [^{125}I]tyramine cellobiose-labeled LDL or albumin followed by a continuous infusion of the same preparation for 4 h. The rate of this continuous infusion was adjusted for the turnover rate of each protein to maintain a constant specific activity in the plasma over the entire infusion (30). Ten minutes before the termination of this continuous infusion, a bolus of ^{131}I-labeled LDL or albumin was administered to each animal to determine the volume of distribution of that particular preparation at time 0. The animals were then exsanguinated at 4 h, and all major organs were removed. The residual carcass, containing principally muscle, bone, and marrow, was homogenized. Tissue and plasma samples were assayed for their content of ^{125}I and ^{131}I. After correcting for the initial volume of distribution of the various radiolabeled proteins, the rates of clearance of each of these probes in the different organs were determined and expressed as microliters of plasma cleared of the particular molecule each hour per gram wet weight of tissue (μl/h/g). When these values were multiplied by the organ weight, the clearance rates per whole organ were obtained (μl/h/organ or μl/day/organ). In the case of the LDL preparations, when these values were multiplied by the concentration of LDL-TC in the plasma, the absolute values for the micrograms of cholesterol taken up each day into each organ were obtained (μg/day/organ). The sum of the clearance rates in all organs gave the whole animal clearance rates, and these values, along with the plasma LDL-TC concentration, could be used to calculate the milligrams of LDL-TC turned over each day by the whole animal per kilogram of body weight (mg/day/kg).

Measurement of plasma and tissue cholesterol concentrations and liver function tests

The plasma total cholesterol concentration was measured enzymatically (kit 1127771; Boehringer Mannheim, Indianapolis, IN). All tissue samples were removed from the animals at the end of the experiments and extracted. The unesterified and esterified

fractions were separated, and the cholesterol in each fraction was then quantitated by gas-liquid chromatography (31–33). These values are presented as amounts of sterol in each whole organ per kilogram of body weight (mg/organ/kg). Plasma liver function tests were measured by a commercial laboratory.

Histological examination of various tissues

At the termination of the experiments, various tissues were removed, fixed in 10% buffered formalin, and embedded in paraffin. These blocks were then sectioned (5 μm thick) and stained with hematoxylin and eosin.

Calculations

The data from all experiments are presented as means ± SEM for the number of animals indicated. Where necessary, differences between mean values were tested for statistical significance ($P < 0.05$) using a two-tailed, unpaired Student's *t*-test (GraphPad Software, Inc., San Diego, CA).

RESULTS

To sort out the various processes that result in the tissue uptake of circulating LDL-TC, the rates of clearance of homologous mouse LDL by the organs of the control $ldlr^{+/+}/npc1^{+/+}$ animals were first measured. As anticipated from previously published work in the rat, hamster, rabbit, and cynomolgus monkey (31, 34, 35), the rates of clearance per gram of tissue were very high (>250 μl/hr/g) in adrenal and liver (**Fig. 2A**), but in all of the remaining organs they were very low (<30 μl/hr/g). Notably, no uptake was detected in the skin or central nervous system. When organ weights (Fig. 2B) and the plasma LDL-TC concentration were taken into consideration, the uptake of cholesterol carried in LDL overwhelmingly took place in the liver. Thus, whereas the whole animal cleared 656 μg of LDL-TC per day (Fig. 2C), the liver accounted for 514 μg/day of this uptake. Of the other organs, only the residual carcass (44 μg/day) and small bowel (35 μg/day) had notable, although much lower, rates of lipoprotein cholesterol uptake. As the residual carcass in this experiment consisted primarily of muscle, bone, and marrow, and because muscle itself takes up virtually no LDL-TC, this finding implied that the cells of the marrow actively used LDL-TC. Assuming that the plasma volume in these mice equaled 60.4 ml/kg body weight (36), the pool of LDL-TC in these animals equaled 4.23 mg/kg, the rate of

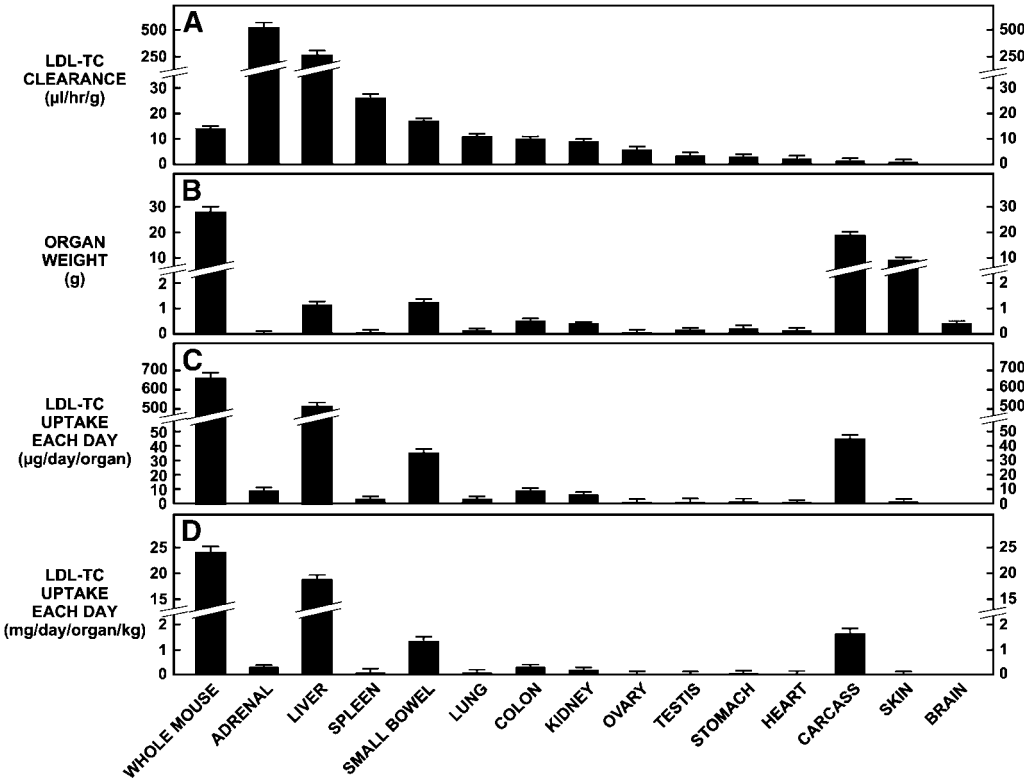

Fig. 2. Total cholesterol carried in LDL (LDL-TC) clearance into the major tissues of the $ldlr^{+/+}/npc1^{+/+}$ mouse. These animals were infused with [^{125}I]tyramine cellobiose-labeled homologous mouse LDL, and rates of lipoprotein uptake were quantitated in the whole animal and in every major organ. A: Rates of uptake expressed as clearance values in microliters of plasma entirely cleared of its LDL-TC content by a given tissue per hour per gram wet weight. B: Mean weights of the whole animal and each major tissue. C: When these clearance values are multiplied by the concentration of LDL-TC in the plasma and by the respective organ weights, the data shown are obtained in micrograms of LDL-TC taken up each day into each organ. D: These same uptake rates normalized to a constant animal body weight of 1 kg. In this experiment, carcass refers to what tissues remain after the other organs are removed. All data represent means ± SEM for measurements made in 11 mice.

LDL-TC turnover was 23 mg/day/kg (Fig. 2D), and the fractional catabolic rate equaled 5.4 pools/day.

These measurements were next repeated in mice in which all LDLR activity had presumably been inactivated (**Fig. 3**). In these animals, the relative clearance of LDL-TC per gram of tissue was reduced markedly in the adrenal and liver but to a much lesser degree in the other organs (Fig. 3A). Although the organ weights in these $ldlr^{-/-}/npc1^{+/+}$ mice were similar to those of the control animals (Fig. 3B), the circulating plasma LDL-TC concentration was 14-fold higher. As a consequence, the relative amounts of LDL-TC taken up in each tissue varied greatly from the values found in the control animals. The mass of LDL-TC cleared by the whole $ldlr^{-/-}/npc1^{+/+}$ animal, for example, was significantly greater (1,109 μg/day) than that in the control mice (656 μg/day) (Fig. 3C), whereas uptake in the liver (411 vs. 514 μg/day) was nearly the same. In many other organs, such as the small bowel (150 vs. 35 μg/day), spleen (29 vs. 3 μg/day), lung (26 vs. 3 μg/day), and residual carcass (392 vs. 44 μg/day), the amount of LDL-TC taken up was actually markedly increased in the animals lacking LDLR activity. Thus, in contrast to the $ldlr^{+/+}/npc1^{+/+}$ mice, the extrahepatic organs became the predominant site for the clearance of LDL-TC. The pool of LDL-TC in these mice was increased to 61.2 mg/kg, the rate of LDL-TC turnover was increased to 41 mg/day/kg (Fig. 3D), and the fractional catabolic rate was decreased to 0.67 pools/day.

From these two sets of data, it appeared that the clearance of LDL-TC by the various organs could be separated into receptor-mediated and receptor-independent (measured in the $ldlr^{-/-}/npc1^{+/+}$ mice) components. The relative importance of the receptor-independent component varied markedly in the different tissues, being very low in the adrenal (1.8% of total clearance) and liver (6.1%) but much higher in organs like spleen (58%), small bowel (35%), lung (63%), and residual carcass (64%). Nevertheless, it was still conceivable that in some manner this apparent receptor-independent component of clearance was the result of residual LDLR activity in the $ldlr^{-/-}/npc1^{+/+}$ animals. To further explore this important issue, studies were next undertaken to identify LDL preparations that could not interact with the mouse LDLR.

As seen in **Fig. 4A**, **C**, **E**, **G**, various tissues of the $ldlr^{+/+}/npc1^{+/+}$ mice cleared ovine LDL from the plasma at higher rates but cleared human LDL at lower rates than these organs cleared homologous mouse LDL. Thus, both of these heterologous LDL preparations still interacted with the LDLR of the mice, albeit at different rates. However, when the human LDL was reductively methylated,

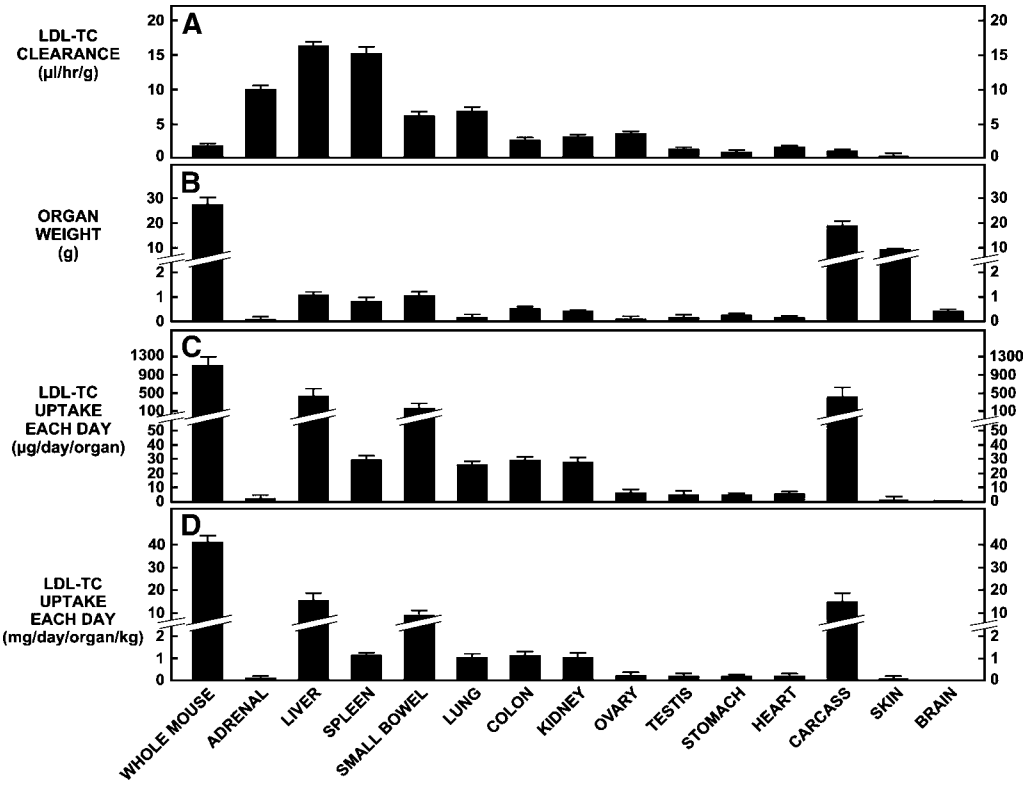

Fig. 3. LDL-TC clearance into the major tissues of the $ldlr^{-/-}/npc1^{+/+}$ mouse. As described in the legend to Fig. 2, these animals were infused with radiolabeled homologous mouse LDL and rates of lipoprotein uptake were quantitated in the whole animal and in every major organ. As in Fig. 2, these uptake rates are represented as clearance values in A, and the weight of each organ is given in B. C illustrates the absolute amount of LDL-TC taken up each day by each organ, and D illustrates the amount of LDL-TC taken up each day into each organ when the animal weight is normalized to 1 kg. All values represent means ± SEM for measurements made in 10 animals.

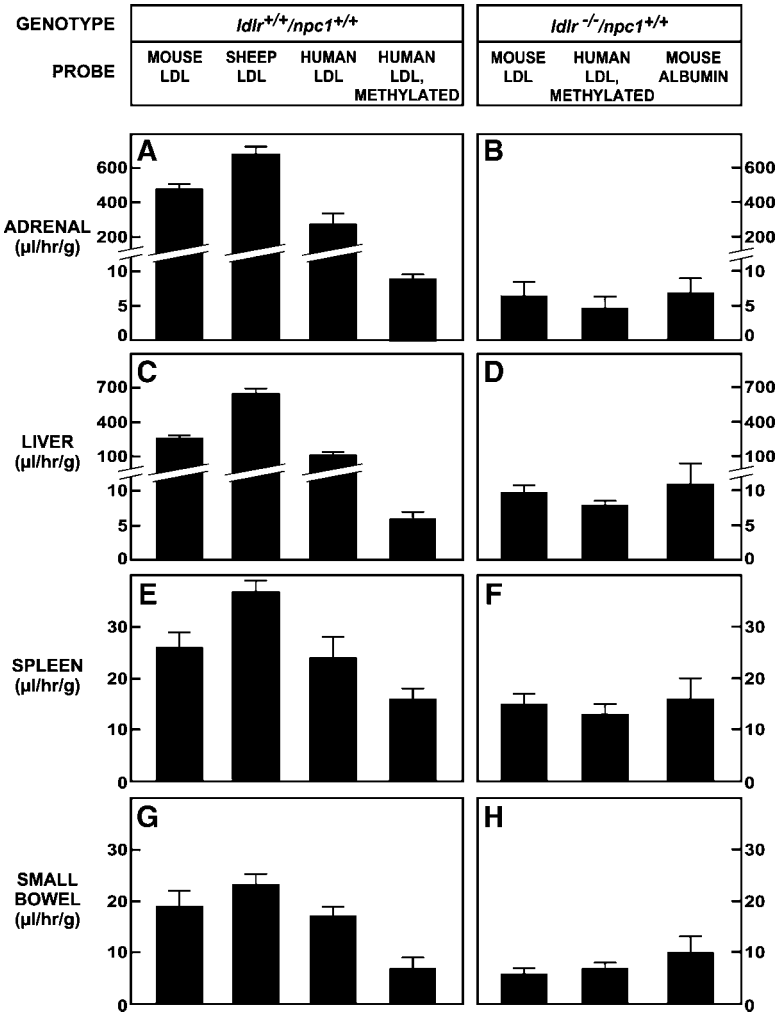

Fig. 4. Rates of clearance of various heterologous and derivatized preparations of LDL. To find an LDL preparation that bound poorly, or not at all, to the mouse low density lipoprotein receptor (LDLR), LDLs of mouse, sheep, and human origin were radiolabeled and infused into both the $ldlr^{+/+}/npc1^{+/+}$ and $ldlr^{-/-}/npc1^{+/+}$ animals. Similar studies were carried out with human LDL that had been reductively methylated to block its interaction with the LDLR. Uptake rates were also measured in the $ldlr^{-/-}/npc1^{+/+}$ animals for mouse albumin. Clearance rates for these various preparations are shown for the adrenal (A, B) and liver (C, D), two organs with very high proportions of receptor-mediated transport, and for the spleen (E, F) and small bowel (G, H), two organs with very low rates of receptor-mediated uptake. Each value represents the mean ± SEM for measurements made in 7–14 animals. In all four organs, there were no significant differences in clearance values of mouse LDL, methylated human LDL, or mouse albumin in the $ldlr^{-/-}/npc1^{+/+}$ animals (B, D, F, H).

clearance in the adrenal decreased from 274 to 9 μl/hr/g (Fig. 4A) and that in the liver decreased from 111 to 6 μl/hr/g (Fig. 4C). In contrast, this reductive methylation only decreased the clearance of the human LDL particle from 24 to 16 μl/hr/g in the spleen (Fig. 4E) and from 17 to 7 μl/hr/g in the small bowel (Fig. 4G), two organs with only a very small apparent component of receptor-mediated uptake. Most importantly, and in contrast to these findings in the control animals, the rates of clearance of homologous mouse LDL and reductively methylated human LDL were virtually identical in all four organs of the $ldlr^{-/-}/npc1^{+/+}$ mice (Fig. 4B, D, F, H). Furthermore, a second indifferent protein, mouse albumin, also was cleared in these organs at the same rates as was the mouse LDL. Thus, these findings strongly supported the conclusion that there was no detectable LDLR activity remaining in the $ldlr^{-/-}/npc1^{+/+}$ mice and that the LDL clearance that was observed in these animals represented bulk-phase endocytosis.

The magnitude of this process could be calculated from the rates of clearance of methylated human LDL in either the $ldlr^{+/+}/npc1^{+/+}$ or $ldlr^{-/-}/npc1^{+/+}$ animals or from the uptake of homologous mouse LDL in the $ldlr^{-/-}/npc1^{+/+}$ animals. In this latter group of mice, for example, the whole animal cleared 1.70 μl of bulk fluid/h/g (Fig. 3A), which equals a clearance rate of 40.8 ml/day/kg body weight. Because the plasma volume in these animals equaled 60.4 ml/kg, this finding implied that nearly two-thirds of the plasma volume was endocytosed every 24 h. Furthermore, the fact that the control animals cleared homologous mouse LDL at a rate of 14.1 μl/hr/g (Fig. 2A), or 338 ml/day/kg, dramatically demonstrated how the binding of LDL to the LDLR and the subsequent concentration and clustering of these complexes into coated pits (Fig. 1A, B) increased by >8-fold the clearance of LDL in the normal mouse (338 ÷ 40.8 ml/day/kg).

Although these conclusions were based upon measurements of LDL clearance using either LDL that was not a ligand for the mouse LDLR or, alternatively, animals that lacked LDLR activity, a second test of this conclusion was possible. The total amount of LDL-TC taken up by both receptor-mediated and bulk-phase endocytosis in any organ equals the product of the clearance rate in that organ and the concentration of LDL-TC in the plasma (Fig. 2C). In any organ like adrenal that relies predominantly on receptor-mediated LDL-TC uptake (98.2% of total), deletion of LDLR activity should decrease the amount of cholesterol reaching the tissue. In contrast, in organs like

spleen and lung that rely much less on receptor-mediated uptake (~40% of total), deletion of LDLR function should greatly increase LDL-TC uptake (Fig. 3C). These predicted differences in the mass uptake of cholesterol through both receptor-mediated and bulk-phase endocytosis could be measured directly in the various tissues of animals lacking NPC1 function, because, in this circumstance, sterol that is endocytosed by either mechanism presumably becomes trapped in the late endosomal/lysosomal compartment (Fig. 1). Thus, based on the differences in the rates of LDL-TC uptake in the various tissues after deletion of LDL function (Fig. 3C vs. Fig. 2C), the amount of unesterified cholesterol trapped in the adrenal should be reduced, that in the liver should be relatively unchanged, and that in extrahepatic organs like lung, spleen, and small bowel should be increased.

As seen in **Fig. 5**, in the absence of NPC1 function in the $ldlr^{+/+}/npc1^{-/-}$ mice, the plasma cholesterol concentration (Fig. 5A), various liver function tests (Fig. 5C–E), and the levels of unesterified cholesterol were all significantly increased compared with those in the control $ldlr^{+/+}/npc1^{+/+}$ mice. This increased content of cholesterol in the whole animal (Fig. 5F) and various organs (Fig. 5G–J) presumably reflected the amount of sterol being taken up by both receptor-mediated and bulk-phase endocytosis through the clathrin-coated pit pathway in these animals with normal LDLR function. However, when the receptor-mediated component of this uptake process was eliminated and the plasma cholesterol concentration increased markedly, as in the $ldlr^{-/-}/npc1^{-/-}$ mice (Fig. 5A), the relative content of unesterified cholesterol in the whole animal (Fig. 5F), spleen (Fig. 5I), and lung (Fig. 5J) increased significantly, mirroring the relative increases in LDL-TC uptake measured directly in these same tissues (Figs. 2C, 3C). Similarly, the decline in the content of cholesterol in the adrenal (Fig. 5G) and the lack of change in the liver (Fig. 5H) also reflected the fact that LDL-TC uptake was reduced in this endocrine organ but was essentially unchanged in the liver (Figs. 2C, 3C).

Two other points concerning this study should be emphasized. First, we have previously shown that liver dysfunction in NPC disease is essentially a linear function of the amount of cholesterol trapped in the liver (37). In this study, deletion of LDLR activity did not further change the content of sterol in the liver (Fig. 5H) and did not further alter the plasma transaminase levels (Fig. 5D, E). Second, in the presence of the NPC1 mutation, nearly all of the cholesterol in the tissues is unesterified (21). The exception is the adrenal, which takes up large amounts of cholesteryl ester carried in HDL by a mechanism that bypasses the block in transport out of the endosomal/lysosomal compartment (24). In the adrenal, where the concentration of unesterified cholesterol decreased significantly with interruption of LDLR function (Fig. 5G), the concentration of cholesteryl ester was normal (data not shown).

As these two sets of data confirmed the validity of the measurements quantitating clearance rates for both receptor-mediated and bulk-phase endocytosis of lipoprotein cholesterol, it was next possible to explore the quantitative nature of the unesterified cholesterol sequestration that takes place in every tissue when NPC1 protein is mutationally inactivated. In **Fig. 6A**, the absolute amount of excess cholesterol that accumulated in the organs of the $ldlr^{+/+}/npc1^{-/-}$ mouse by 56 days of age is shown by the

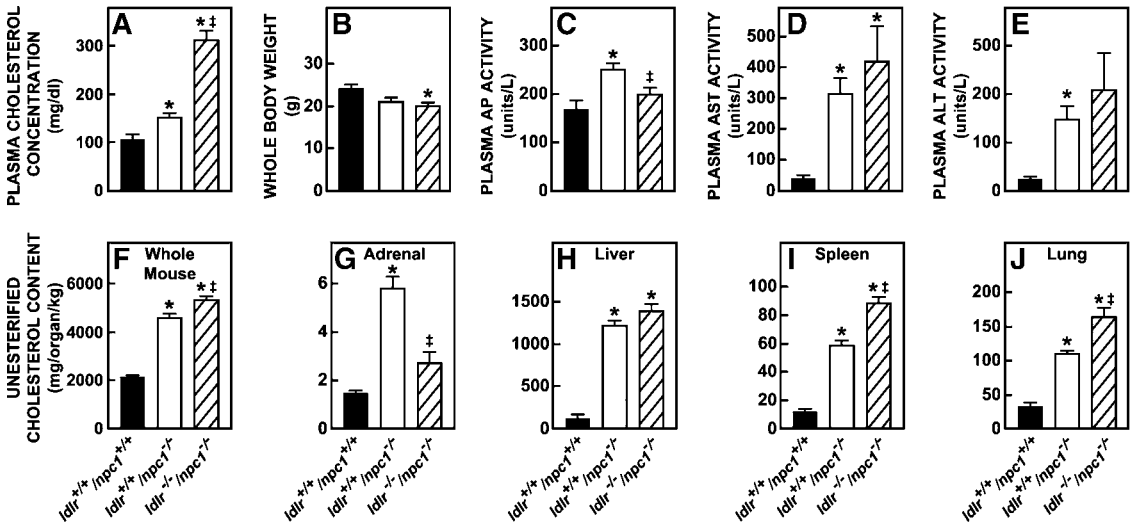

Fig. 5. Effect of deleting LDLR activity on the accumulation of unesterified cholesterol in various tissues of the animals lacking NPC1 function. In this study, three groups of animals genotyped as $ldlr^{+/+}/npc1^{+/+}$, $ldlr^{+/+}/npc1^{-/-}$, and $ldlr^{-/-}/npc1^{-/-}$ were maintained on the low-cholesterol diet and euthanized at 56 days of age, when measurements of plasma total cholesterol concentration (A), whole body weight (B), and various liver function tests (C–E) were made. In addition, the content of unesterified cholesterol was also determined in the whole mouse (F) as well as in the adrenal (G), liver (H), spleen (I), and lung (J). These values are presented as milligrams of sterol present in each organ per kilogram of body weight. Each value represents the mean ± SEM for measurements made in 8–11 animals. * $P < 0.05$ compared with the control $ldlr^{+/+}/npc1^{+/+}$ animals; ‡ $P < 0.05$ compared with the $ldlr^{+/+}/npc1^{-/-}$ animals. AP, alkaline phosphatase; ALT, alanine aminotransferase; AST, aspartate aminotransferase.

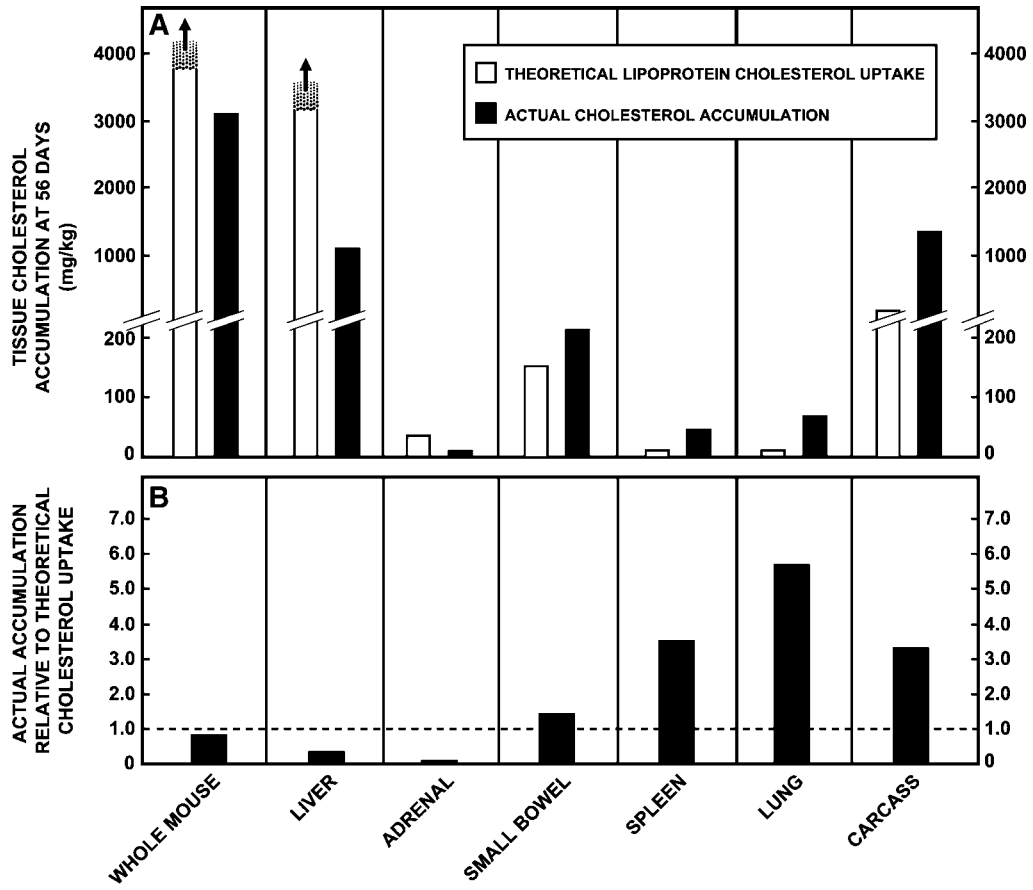

Fig. 6. Theoretical and actual rates of cholesterol accumulation in the tissues of the $ldlr^{+/+}/npc1^{-/-}$ mouse. Both $ldlr^{+/+}/npc1^{+/+}$ and $ldlr^{+/+}/npc1^{-/-}$ animals were maintained on the low-cholesterol diet and euthanized at 56 days of age. The mass of unesterified cholesterol present in the whole animal and in various organs was determined and expressed as milligrams per kilogram of body weight. This mass of sterol found in the $ldlr^{+/+}/npc1^{-/-}$ mouse minus the mass found in the control animal represented the amount of excess cholesterol that accumulated in the mutant animal over 56 days as a result of the NPC1 mutation. These values are shown as closed bars in A. The open bars represent the theoretical amount of cholesterol that should have accumulated over this period based on rates of lipoprotein cholesterol uptake. The theoretical value shown for the whole mouse represents the sum of all of the LDL-TC cleared (2,856 mg/kg) and the dietary cholesterol absorbed (896 mg/kg) during this period, whereas the value for the liver equals the sum of that portion of the LDL-TC pool taken up (2,240 mg/kg) and the dietary cholesterol absorbed (896 mg/kg). As indicated, these two values are underestimates of the theoretical value to the extent that clearance rates for the very low density lipoprotein remnant (VLDLr) and biliary cholesterol absorbed through the intestine were not available. The theoretical rates for the other organs were calculated solely from their rates of LDL-TC clearance (see Fig. 2), assuming that chylomicron remnant and VLDLr were not take up by these organs. In B, the actual observed amounts of cholesterol accumulated in the tissues were divided by the respective theoretical amounts that should be present based upon these rates of lipoprotein clearance. In this experiment, carcass refers to what tissues remained after the other organs were removed. The actual rates of accumulation were derived from two groups of animals, each containing 10 animals each.

closed bars and is expressed as milligrams of sterol per kilogram of body weight. At this age, the whole mutant mouse had accumulated an excess of 3,100 mg/kg cholesterol compared with the control animal, whereas 1,102 mg/kg of this excess was found in the liver. Lesser amounts accumulated in organs like small bowel, spleen, lung, and carcass (presumably largely in marrow cells). For comparison, the open bars show the amount of lipoprotein cholesterol that should have been taken up by both receptor-mediated and bulk-phase endocytosis and trapped in these tissues during the 56 day period. These theoretical values were calculated using the clearance data that had just been determined (see legend).

As is apparent, in the whole mouse the actual accumulation of sterol was close to the minimal theoretical value (3,100 vs. 3,752 mg/kg), whereas accumulation in the liver was much lower than predicted (1,102 vs. 3,136 mg/kg). In contrast, although the extrahepatic organs accumulated much less sterol than the liver over this period, in many organs this accumulation was greater than predicted from

the rates of LDL-TC uptake. This is emphasized in Fig. 6B, in which actual sterol accumulation over 56 days was shown to be 3- to 6-fold greater than predicted in organs like spleen, lung, and carcass. Conceivably, this difference in the accumulation of cholesterol in some extrahepatic organs, compared with the liver, reflected an unexpected shift in the clearance of lipoproteins like the CMr to the periphery in the mutant animals. This was not the case, however, because treatment of the $ldlr^{+/+}/npc1^{-/-}$ mouse with ezetimibe to block cholesterol absorption decreased sterol accumulation in the liver from 1,207 to 742 mg/kg but had essentially no effect on accumulation in the peripheral organs. Furthermore, when these studies were repeated in animals also lacking LDLR function, accumulation in the liver was essentially unchanged (1,260 vs. 1,207 mg/kg), whereas accumulation in tissues like the spleen (95 vs. 65 mg/kg) and lung (149 vs. 109 mg/kg) was increased. Thus, in the presence of the NPC1 mutation, there was exaggerated cholesterol accumulation in a number of extrahepatic organs, and bulk-phase endocytosis played an important role in this accumulation.

These findings raised the question of whether there were morphological alterations in some organs of the $ldlr^{+/+}/npc1^{-/-}$ mouse that could account for this excessive and unpredicted accumulation of cholesterol. As illustrated in **Fig. 7**, in several organs, like skeletal and cardiac

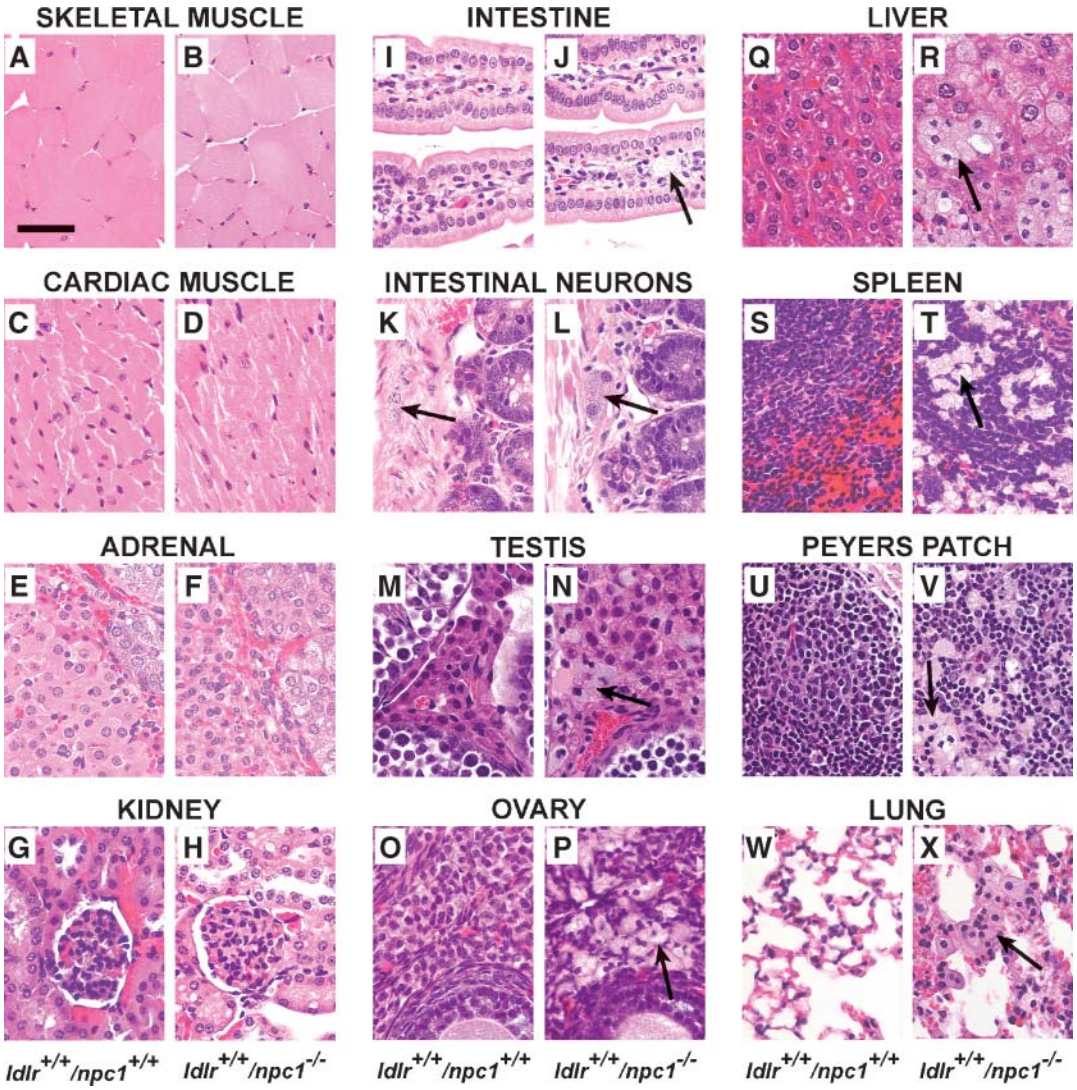

Fig. 7. Comparison of the histopathology of the major organs of the $ldlr^{+/+}/npc1^{+/+}$ and $ldlr^{+/+}/npc1^{-/-}$ mice. To examine the histological alterations that might have occurred in the presence of the NPC1 mutation (see Fig. 6), tissue sections were prepared and stained with hematoxylin and eosin. These pairs of tissue samples are arranged beginning with those manifesting no histopathology (A–H), those with modest changes (I–P), and, finally, those with marked abnormalities (Q–X). In J–X, the arrows point to histological abnormalities found in certain tissues and described in the text. Each panel is a representative section taken from the different animals, and all were photographed at the same magnification. Bar = 40 μm.

muscle, adrenal, and kidney, no histological changes were evident (Fig. 7A–H). The morphology of the small intestine also was essentially normal except for the presence of an occasional foamy macrophage in the villous core (Fig. 7J) and a vesicular transformation of the cytosol in the autonomic neurons (Fig. 7L) that was similar to changes seen in the neurons and glial cells of the central nervous system in the $ldlr^{+/+}/npc1^{-/-}$ mouse (38). Both the testis (Fig. 7N) and ovary (Fig. 7P) also revealed similar histologic abnormalities. However, the most marked changes were seen in those organs that typically have large numbers of macrophages and are part of the reticuloendothelial system. Clusters of foamy macrophages were scattered throughout the liver and interspersed with swollen hepatocytes with vesicular cytoplasmic changes (Fig. 7R). Similar macrophage invasion was found in the spleen (Fig. 7T) and mucosa-associated lymphoid collections in Peyer's patches (Fig. 7V). Most striking was the lung, which showed marked accumulation of foamy macrophages within alveoli and apparent reduction in air spaces (Fig. 7X). Presumably, there were similar collections of macrophages in the marrow, but this was not examined specifically. Thus, some of those same organs with the greatest unpredicted rates of cholesterol accumulation at 56 days of age (Fig. 6B) seemed to have the greatest degree of macrophage infiltration (Fig. 7).

In a final experiment, the degree to which these morphological changes were dictated by the amount of LDL-TC taken up and trapped within the late endosomal/lysosomal compartment was explored. As established earlier, deletion of LDLR function had little effect on LDL-TC uptake in the liver (411 vs. 514 μg/day) but increased uptake in the extrahepatic organs (698 vs. 142 μg/day) in general and in the spleen and lung (Figs. 2, 3) in particular. However, this shift in cholesterol uptake did not alter the morphology of these tissues. As shown in **Fig. 8**, there was no macrophage infiltration and no vesicular transformation of the cytosol in the cells of the adrenal (Fig. 8A, B), liver (Fig. 8E, F), spleen (Fig. 8I, J), or lung (Fig. 8M, N) in the $ldlr^{-/-}/npc1^{+/+}$ mice compared with the control $ldlr^{+/+}/npc1^{+/+}$ animals. Similarly, in the adrenal, which primarily uses cholesterol derived from HDL and not LDL-TC (24), tissue morphology also was essentially unchanged in the $ldlr^{+/+}/npc1^{-/-}$ (Fig. 8C) and $ldlr^{-/-}/npc1^{-/-}$ (Fig. 8D) mice. However, in the animals with these same genotypes, there were striking differences in morphology in those tissues that actively took up LDL-TC through receptor-mediated and bulk-phase endocytosis. In the absence of NPC1 function, there were clusters of foamy macrophages scattered throughout the liver (Fig. 8G), and the density of these collections was about the same when LDLR function was also ablated (Fig. 8H). This infiltration of macrophages was more pronounced in the spleen (Fig. 8K) and lung (Fig. 8O) of the $ldlr^{+/+}/npc1^{-/-}$ mice, and in contrast to the liver, the degree of infiltration was much more pronounced in the $ldlr^{-/-}/npc1^{-/-}$ animals (Fig. 8L, P). Thus, the severity of the macrophage infiltration appeared to correlate with the magnitude of LDL-TC uptake in these organs, even though this uptake in the $ldlr^{-/-}/npc1^{-/-}$ mice was entirely through bulk-phase endocytosis.

DISCUSSION

Mutational inactivation of the transporter NPC1 leads to cellular dysfunction in virtually every tissue in the body. Clinically, in the human, this cellular abnormality may be expressed as severe liver disease, pulmonary failure, chronic diarrhea, or progressive neurological disease (39–42). The biochemical hallmark of this syndrome is an age-related, progressive accumulation of unesterified cholesterol in the cells of every organ (21, 33, 43). This sequestered sterol is derived from various lipoproteins taken up into the cells by both receptor-mediated and bulk-phase endocytosis through clathrin-coated pits and is manifest histologically as vesicular lipid accumulation throughout the cytosolic compartment (38, 43, 44). In a number of organs, including liver, lymphoid tissue, lung, and brain, there is also infiltration and activation of macrophages (glia, in the case of the central nervous system), which may play a role in the death of cells in each of these organs (Fig. 8) (33, 45, 46). Furthermore, when more lipoprotein cholesterol is shifted to some of these extrahepatic organs, there is apparently an increase in this infiltration of macrophages. These studies raise important issues with respect to the role of this cholesterol accumulation in parenchymal cells, as opposed to macrophage infiltration, in initiating cell death and, hence, the development of clinical symptoms in this genetic disorder.

LDLRs are expressed in many tissues, including cells of the central nervous system, and bind lipoproteins containing apoE with high affinity but those with apoB-100 with lesser affinity (2, 47–49). However, access to these receptors is limited by the permeability characteristics of the endothelial barriers in each organ (Fig. 1), a fact that probably accounts for the observation that nearly all CMr and VLDLr particles and 70–80% of LDL particles are cleared from the plasma by the liver, an organ with a fenestrated sinusoidal capillary system (5). Only 20–30% of the plasma LDL-TC pool normally is cleared by the extrahepatic organs in most species, including humans, although none is taken up into the central nervous system (3, 22, 50). As this process of receptor-mediated endocytosis involves interaction of the LDL particles with a finite number of receptor sites on the liver, the rate of LDL-TC uptake manifests saturation kinetics with respect to the concentration of this lipoprotein in the plasma (34). However, because the apoE-containing CMr and VLDLr particles bind more effectively, and so compete with the binding of the LDL particles, the apparent Michaelis constant for the uptake of LDL-TC is shifted to much higher values than would be true in the absence of such apoE-containing lipoproteins (7). As a consequence, the steady-state concentration of LDL-TC in the plasma is typically much higher than the steady-state levels of CMr and VLDLr.

Apart from this receptor-mediated process, these same cells, including macrophages, typically engulf small vol-

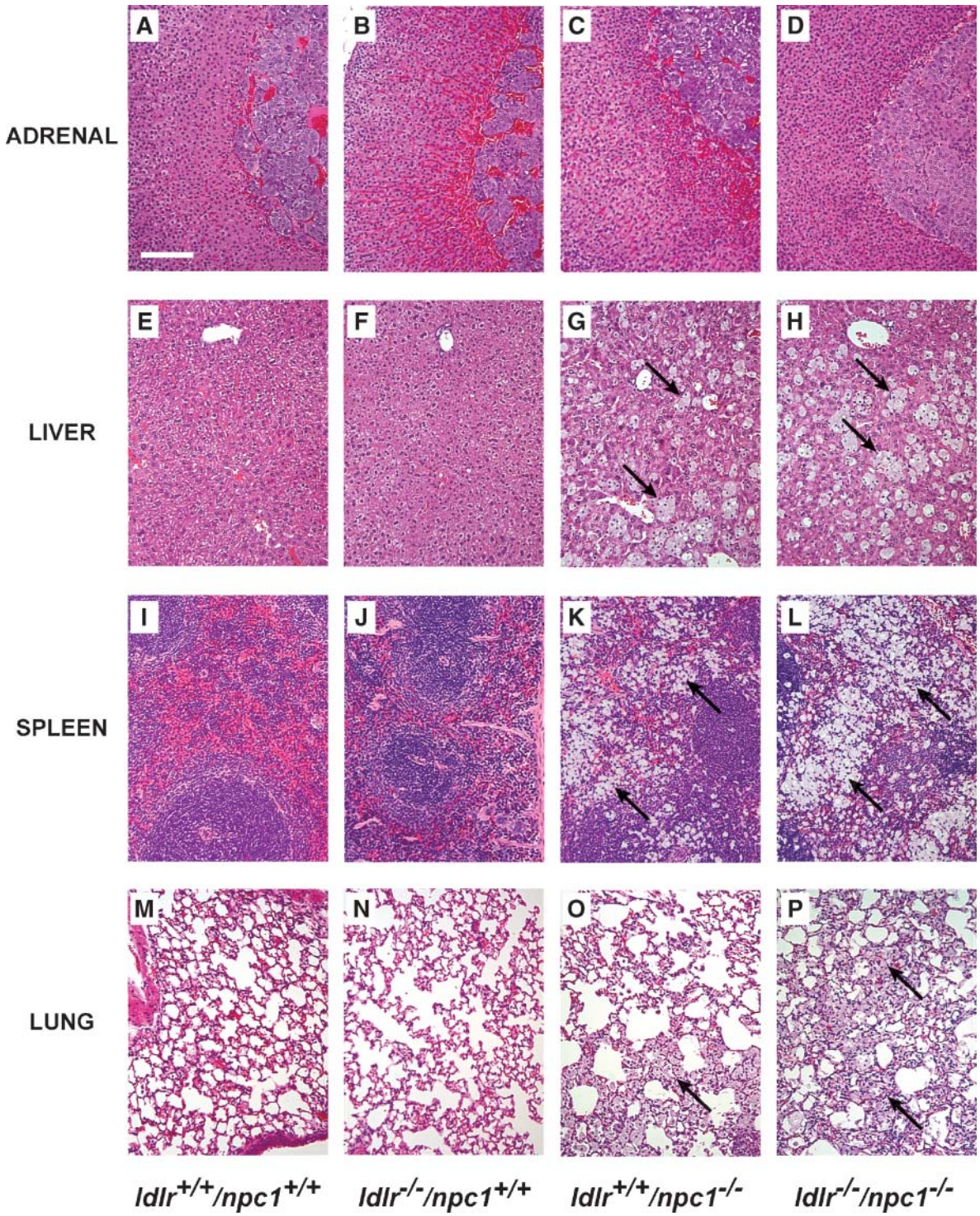

Fig. 8. Macrophage infiltration of various organs in the mouse lacking NPC1 function. Representative histological sections of four organs from control animals (A, E, I, M), animals lacking the LDLR (B, F, J, N), animals with the NPC1 mutation (C, G, K, O), and animals lacking both LDLR and NPC1 function (D, H, L, P) are shown. The arrows in panels G, H, K, L, O, and P point to clusters of pale-staining, foamy macrophages. All of these sections were photographed at the same magnification. Bar = 100 μm.

umes of bulk pericellular fluid during invagination of the endocytotic vesicles that typically are 80–200 nm in diameter (Fig. 1). Because LDL particles are present in this pericellular fluid, this bulk-phase endocytosis represents a second, receptor-independent, process for the uptake of LDL-TC into the cells. The magnitude of such uptake can be measured using homologous LDL in mice lacking LDLRs, derivatized LDL that cannot bind to the LDLR, or indifferent probe molecules such as albumin, inulin, or sucrose. In the current studies, three different methods

were used, and all gave essentially the same values (Fig. 4B, D, F, H). It should be noted that because the rate of uptake by this process does not involve interaction with a finite number of receptor sites, but is proportional to the concentration of LDL-TC in the pericellular fluid, the kinetics of this uptake process are linear and not saturable (34). As expected, clearance of the LDL particles from the plasma by this bulk-phase process was much lower in the whole mouse (46 μl/h; Fig. 3A) than it was in the animals in which receptor-mediated endocytosis was the predominant transport mechanism (391 μl/h; Fig. 2A).

However, because the rate of receptor-mediated LDL-TC uptake is saturable and that of bulk-phase endocytosis is a linear function of the plasma lipoprotein concentration, more LDL-TC is actually taken up and degraded in the absence of LDLRs than in the presence of these receptors. In this study, for example, the $ldlr^{-/-}/npc1^{+/+}$ mice took up 41 mg/day/kg (Fig. 3D) LDL-TC compared with 23 mg/day/kg removed from the plasma by the control $ldlr^{+/+}/npc1^{+/+}$ animals (Fig. 2D). Similarly enhanced LDL-TC turnover has been reported in the rabbit (105 vs. 19 mg/day/kg) and human (40 vs. 13 mg/day/kg) lacking functional LDLRs (22, 35). In these situations, the VLDLr particles are apparently removed more slowly from the plasma by the liver so that a greater percentage of these particles is converted to LDL. As a result, although less cholesterol is returned to the liver as VLDLr, more is cleared from the plasma as LDL-TC. Thus, in familial hypercholesterolemia, although there is expansion of the pool of cholesterol in the plasma, sterol levels and turnover in the tissues are essentially normal, as is the histology of the major organs (Fig. 8B, F, J, N) (17, 18, 30).

These studies reveal that both receptor-mediated and bulk-phase endocytosis contribute to the age-related expansion of the unesterified cholesterol pool in the late endosomal/lysosomal compartment of the parenchymal cells in all tissues of the NPC animals. Because LDL-TC uptake from the plasma in the whole mouse (656 μg/day; Fig. 2C) takes place predominantly in the liver (514 μg/day; Fig. 2C), it is not surprising that this organ accounts for a major portion of the progressive expansion of the whole-body cholesterol pool seen in NPC disease (Fig. 5F, H) (21, 33). Furthermore, this expansion is associated with an increase in relative liver size, infiltration of this organ with foamy macrophages (Fig. 7R), vesicular lipid inclusions in swollen hepatocytes, evidence of cellular death through apoptosis, and abnormal liver function tests (Fig. 5C–E) (33). The amount of cholesterol sequestered in the liver of 56 day old mice can be varied over a range of ~15–90 mg by manipulation of the amount of cholesterol absorbed across the intestine and carried to the liver in the CMr (37). Importantly, the severity of liver damage in such animals, as assessed by liver function tests, varies directly with the amount of cholesterol reaching the cells of this organ and becoming entrapped within the late endosomal/lysosomal compartment.

More surprisingly, however, were the findings in several extrahepatic organs. Unlike the liver, in which only ~6% of LDL-TC uptake was through bulk-phase endocytosis, in tissues like the spleen, lung, and carcass (i.e., marrow), nearly two-thirds of uptake was normally through bulk-phase endocytosis, even in the $ldlr^{+/+}/npc1^{+/+}$ mice. Furthermore, the amount of cholesterol sequestered in these tissues in the $ldlr^{+/+}/npc1^{-/-}$ animals was three to six times greater (Fig. 6B) than predicted from the rate constants for LDL-TC uptake measured in the control mice (Fig. 2C). Like the liver, several of these organs were enlarged relative to body weight and heavily infiltrated with macrophages (Fig. 8K,O) (45). This finding raised the possibility, therefore, that much of the unpredicted sequestration of cholesterol found in these organs came about because of LDL-TC clearance by the infiltrating macrophages as well as the parenchymal cells of the respective organs. As an aside, this same infiltration of lipid-laden macrophages is seen in the lungs of children with NPC disease and is described pathologically as "lipoid pneumonitis" (41).

That these macrophages play a role in NPC disease is further supported by the observation that both the cholesterol accumulation and cellular infiltration were made worse when more lipoprotein cholesterol uptake was induced in these tissues. With deletion of LDLR function, LDL-TC uptake remained about the same in the liver (411 vs. 514 μg/day; Figs. 2,3), whereas uptake in the extrahepatic organs increased (698 vs. 142 μg/day; Figs. 2, 3). Under these circumstances, hepatic cholesterol content (Fig. 5H), the degree of macrophage infiltration (Fig. 8H), and the liver function abnormalities (Fig. 5D, E) remained unchanged. In these same animals, however, LDL-TC uptake was increased markedly in tissues like spleen (29 vs. 3 μg/day), lung (26 vs. 3 μg/day), and carcass (392 vs. 44 μg/day) (Figs. 2, 3). Importantly, this enhanced uptake was associated with increased cholesterol accumulation (Fig. 5I, J) and greater apparent macrophage infiltration (Fig. 8L, P). Thus, just as the severity of the liver disease could be varied by altering the amount of cholesterol reaching the hepatocytes through receptor-mediated uptake of the CMr, so also the severity of the histopathology in other organs like lung and lymphoid tissue could be made worse by increasing cholesterol uptake through bulk-phase endocytosis of LDL-TC.

These biochemical and histopathological findings in the liver and extrahepatic tissues are similar to those reported in the central nervous system in NPC disease. Although various members of the LDLR family are expressed in cells of the brain, the movement of cholesterol from glial cells to neurons probably takes place through sterol bound to apoE (49, 51–53). In the NPC mouse, there is accumulation of cholesterol in neurons and glial cells, activation of microglia, the central nervous system equivalent of macrophages, and, ultimately, death of selected populations of neurons and glia (38, 43, 45, 54, 55). However, neither varying the level of cholesterol absorption across the intestine, which alters the severity of the liver disease, nor manipulation of the level of LDLR activity, which alters the severity of the histopathology in tissues like lung, has any effect on this neurodegeneration. NPC mice fed cholesterol or ezetimibe, or subjected to deletion

of LDLR activity, all die a neurological death at about the same age (~76–85 days) as untreated NPC mutants (37, 38, 45) However, several other experimental manipulations are now available that do change cholesterol flux across the central nervous system, and these manipulations alter longevity. Thus, it now appears to be generally true that manipulations that change the flux of cholesterol into and out of various tissues alter the severity of the histopathology in the target organs.

These studies also raise the possibility that the infiltrating and activated macrophages may play a role in the death of the parenchymal cells in these various tissues. However, little is known about the signals that lead to the proliferation of these cells in NPC disease. On the one hand, cholesterol accumulating in the late endosomal/lysosomal compartment of the parenchymal cells might cause these tissues to release trophic factors that induce macrophage migration and activation. On the other hand, it is conceivable that the block in cholesterol trafficking present in the macrophages themselves may lead to these histological abnormalities. In any event, it would be of considerable interest to determine whether the phenotype of the NPC mouse is altered under circumstances in which macrophage migration and proliferation are suppressed.

One final observation that comes from these studies has to do with the magnitude of the movement of unesterified cholesterol out of the late endosomal/lysosomal compartment in the absence of NPC1 activity. Fibroblasts from NPC patients readily accumulate unesterified cholesterol when incubated with LDL (56–58). However, this accumulation of sterol is slowly lost when such fibroblasts are returned to lipoprotein-free medium. A similar "leak" of unesterified cholesterol from this compartment was apparently observed in some organs of the NPC mice in these studies. Based on rates of clearance of the various lipoprotein particles containing apoE and apoB-100, the whole mouse by 56 days of age should have sequestered in excess of 3,752 mg/kg sterol (Fig. 6A). Although several extrahepatic organs accumulated more sterol than expected, the amount of cholesterol sequestered in the liver (1,102 mg/kg) was well below the predicted value (3,136 mg/kg) (Fig. 6A). Thus, it is conceivable that in this organ there was activation of a secondary mechanism for slowly moving some of the sequestered sterol out of the late endosomal/lysosomal compartment to the metabolically active pool in the cytosol. Alternatively, it is also possible that this leak reflected the damage and death of hepatocytes that apparently continuously occurs in this syndrome (37). Which of these two possibilities explains the lower than predicted level of cholesterol in the liver remains to be elucidated.

The authors thank Brian Griffith, Heather Waddell, and Thien Tran for their excellent technical assistance and Kerry Foreman for expert preparation of the manuscript. This work was supported by U.S. Public Health Service Research Grant R01 HL-09610 and U.S. Public Health Service Training Grant T32 DK-07745 and by a grant from the Moss Heart Fund.

REFERENCES

1. Havel, R. J. 1986. Functional activities of hepatic lipoprotein receptors. *Annu. Rev. Physiol.* **48:** 119–134.
2. Kowal, R. C., J. Herz, K. H. Weisgraber, R. W. Mahley, M. S. Brown, and J. L. Goldstein. 1990. Opposing effects of apolipoproteins E and C on lipoprotein binding to low density lipoprotein receptor-related protein. *J. Biol. Chem.* **265:** 10771–10779.
3. Quan, G., C. Xie, J. M. Dietschy, and S. D. Turley. 2003. Ontogenesis and regulation of cholesterol metabolism in the central nervous system of the mouse. *Dev. Brain Res.* **146:** 87–98.
4. Dietschy, J. M., and S. D. Turley. 2004. Cholesterol metabolism in the central nervous system during early development and in the mature animal. *J. Lipid Res.* **45:** 1375–1397.
5. Wright, P. L., K. F. Smith, W. A. Day, and R. Fraser. 1983. Small liver fenestrae may explain the susceptibility of rabbits to atherosclerosis. *Arteriosclerosis.* **3:** 344–348.
6. Ishibashi, S., J. Herz, N. Maeda, J. L. Goldstein, and M. S. Brown. 1994. The two-receptor model of lipoprotein clearance: tests of the hypothesis in "knockout" mice lacking the low density lipoprotein receptor, apolipoprotein E, or both proteins. *Proc. Natl. Acad. Sci. USA.* **91:** 4431–4435.
7. Woollett, L. A., Y. Osono, J. Herz, and J. M. Dietschy. 1995. Apolipoprotein E competitively inhibits receptor-dependent low density lipoprotein uptake by the liver but has no effect on cholesterol absorption or synthesis in the mouse. *Proc. Natl. Acad. Sci. USA.* **92:** 12500–12504.
8. Rudenko, G., L. Henry, K. Henderson, K. Ichtchenko, M. S. Brown, J. L. Goldstein, and J. Deisenhofer. 2002. Structure of the LDL receptor extracellular domain at endosomal pH. *Science.* **298:** 2353–2358.
9. Liou, H. L., S. S. Dixit, S. Xu, G. S. Tint, A. M. Stock, and P. Lobel. 2006. NPC2, the protein deficient in Niemann-Pick C2 disease, consists of multiple glycoforms that bind a variety of sterols. *J. Biol. Chem.* **281:** 36710–36723.
10. Naureckiene, S., D. E. Sleat, H. Lackland, A. Fensom, M. T. Vanier, R. Wattiaux, M. Jadot, and P. Lobel. 2000. Identification of *HE1* as the second gene of Niemann-Pick C disease. *Science.* **290:** 2298–2301.
11. Loftus, S. K., J. A. Morris, E. D. Carstea, J. Z. Gu, C. Cummings, A. Brown, J. Ellison, K. Ohno, M. A. Rosenfeld, D. A. Tagle, et al. 1997. Murine model of Niemann-Pick C disease: mutation in a cholesterol homeostasis gene. *Science.* **277:** 232–235.
12. Blanchette-Mackie, E. J. 2000. Intracellular cholesterol trafficking: role of the NPC1 protein. *Biochim. Biophys. Acta.* **1486:** 171–183.
13. Cheruku, S. R., Z. Xu, R. Dutia, P. Lobel, and J. Storch. 2006. Mechanism of cholesterol transfer from the Niemann-Pick type C2 protein to model membranes supports a role in lysosomal cholesterol transport. *J. Biol. Chem.* **281:** 31594–31604.
14. Walkley, S. U., and K. Suzuki. 2004. Consequences of NPC1 and NPC2 loss of function in mammalian neurons. *Biochim. Biophys. Acta.* **1685:** 48–62.
15. Repa, J. J., and D. J. Mangelsdorf. 2000. The role of orphan nuclear receptors in the regulation of cholesterol homeostasis. *Annu. Rev. Cell Dev. Biol.* **16:** 459–481.
16. Horton, J. D., J. L. Goldstein, and M. S. Brown. 2002. SREBPs: activators of the complete program of cholesterol and fatty acid synthesis in the liver. *J. Clin. Invest.* **109:** 1125–1131.
17. Osono, Y., L. A. Woollett, J. Herz, and J. M. Dietschy. 1995. Role of the low density lipoprotein receptor in the flux of cholesterol through the plasma and across the tissues of the mouse. *J. Clin. Invest.* **95:** 1124–1132.
18. Dietschy, J. M., T. Kita, K. E. Suckling, J. L. Goldstein, and M. S. Brown. 1983. Cholesterol synthesis in vivo and in vitro in the WHHL rabbit, an animal with defective low density lipoprotein receptors. *J. Lipid Res.* **24:** 469–480.
19. Du, H., M. Heur, M. Duanmu, G. A. Grabowski, D. Y. Hui, D. P. Witte, and J. Mishra. 2001. Lysosomal acid lipase-deficient mice: depletion of white and brown fat, severe hepatosplenomegaly, and shortened life span. *J. Lipid Res.* **42:** 489–500.
20. Du, H., M. Duanmu, D. Witte, and G. A. Grabowski. 1998. Targeted disruption of the mouse lysosomal acid lipase gene: long-term survival with massive cholesteryl ester and triglyceride storage. *Hum. Mol. Genet.* **7:** 1347–1354.
21. Xie, C., S. D. Turley, P. G. Pentchev, and J. M. Dietschy. 1999. Cholesterol balance and metabolism in mice with loss of function of Niemann-Pick C protein. *Am. J. Physiol.* **276:** E336–E344.

22. Dietschy, J. M., S. D. Turley, and D. K. Spady. 1993. Role of liver in the maintenance of cholesterol and low density lipoprotein homeostasis in different animal species, including humans. *J. Lipid Res.* **34:** 1637–1659.
23. Xie, C., S. D. Turley, and J. M. Dietschy. 1999. Cholesterol accumulation in tissues of the Niemann-Pick type C mouse is determined by the rate of lipoprotein-cholesterol uptake through the coated-pit pathway in each organ. *Proc. Natl. Acad. Sci. USA.* **96:** 11992–11997.
24. Xie, C., J. A. Richardson, S. D. Turley, and J. M. Dietschy. 2006. Cholesterol substrate pools and steroid hormone levels are normal in the face of mutational inactivation of NPC1 protein. *J. Lipid Res.* **47:** 953–963.
25. Ishibashi, S., M. S. Brown, J. L. Goldstein, R. D. Gerard, R. E. Hammer, and J. Herz. 1993. Hypercholesterolemia in low density lipoprotein receptor knockout mice and its reversal by adenovirus-mediated gene delivery. *J. Clin. Invest.* **92:** 883–893.
26. Glass, C. K., R. C. Pittman, G. A. Keller, and D. Steinberg. 1983. Tissue sites of degradation of apoprotein A-I in the rat. *J. Biol. Chem.* **258:** 7161–7167.
27. Pittman, R. C., T. E. Carew, C. K. Glass, S. R. Green, C. A. Taylor, and A. D. Attie. 1983. A radioiodinated, intracellularly trapped ligand for determining the sites of plasma protein degradation in vivo. *Biochem. J.* **212:** 791–800.
28. Weisgraber, K. H., and R. W. Mahley. 1980. Subfractionation of human high density lipoprotein by heparin-Sepharose affinity chromatography. *J. Lipid Res.* **21:** 316–325.
29. Weisgraber, K. H., T. L. Innerarity, and R. W. Mahley. 1978. Role of the lysine residues of plasma lipoproteins in high affinity binding to cell surface receptors on human fibroblasts. *J. Biol. Chem.* **253:** 9053–9062.
30. Spady, D. K., D. W. Bilheimer, and J. M. Dietschy. 1983. Rates of receptor-dependent and -independent low density lipoprotein uptake in the hamster. *Proc. Natl. Acad. Sci. USA.* **80:** 3499–3503.
31. Turley, S. D., D. K. Spady, and J. M. Dietschy. 1995. Role of liver in the synthesis of cholesterol and the clearance of low density lipoproteins in the cynomolgus monkey. *J. Lipid Res.* **36:** 67–79.
32. Hamilton, J. G., and K. Comai. 1988. Rapid separation of neutral lipids, free fatty acids and polar lipids using prepacked silica Sep-Pak columns. *Lipids.* **23:** 1146–1149.
33. Beltroy, E. P., J. A. Richardson, J. D. Horton, S. D. Turley, and J. M. Dietschy. 2005. Cholesterol accumulation and liver cell death in the mouse with Niemann-Pick type C disease. *Hepatology.* **42:** 886–893.
34. Spady, D. K., J. B. Meddings, and J. M. Dietschy. 1986. Kinetic constants for receptor-dependent and receptor-independent low density lipoprotein transport in the tissues of the rat and hamster. *J. Clin. Invest.* **77:** 1474–1481.
35. Spady, D. K., M. Huettinger, D. W. Bilheimer, and J. M. Dietschy. 1987. Role of receptor-independent low density lipoprotein transport in the maintenance of tissue cholesterol balance in the normal and WHHL rabbit. *J. Lipid Res.* **28:** 32–41.
36. Riches, A. C., J. G. Sharp, D. B. Thomas, and S. V. Smith. 1973. Blood volume determination in the mouse. *J. Physiol.* **228:** 279–284.
37. Beltroy, E. P., B. Liu, J. M. Dietschy, and S. D. Turley. 2007. Lysosomal unesterified cholesterol content correlates with liver cell death in murine Niemann-Pick type C disease. *J. Lipid Res.* **48:** 869–881.
38. Xie, C., D. K. Burns, S. D. Turley, and J. M. Dietschy. 2000. Cholesterol is sequestered in the brains of mice with Niemann-Pick type C disease but turnover is increased. *J. Neuropathol. Exp. Neurol.* **59:** 1106–1117.
39. Mieli-Vergani, G., E. R. Howard, and A. P. Mowat. 1991. Liver disease in infancy: a 20 year perspective. *Gut.* **(Suppl.):** 123–128.
40. Kelly, D. A., B. Portmann, A. P. Mowat, S. Sherlock, and B. D. Lake. 1993. Niemann-Pick disease type C: diagnosis and outcome in children, with particular reference to liver disease. *J. Pediatr.* **123:** 242–247.
41. Palmeri, S., P. Tarugi, F. Sicurelli, R. Buccoliero, A. Malandrini, M. M. De Santi, G. Marciano, C. Battisti, M. T. Dotti, S. Calandra, et al. 2005. Lung involvement in Niemann-Pick disease type C1: improvement with bronchoalveolar lavage. *Neurol. Sci.* **26:** 171–173.
42. Vanier, M. T., and K. Suzuki. 1998. Recent advances in elucidating Niemann-Pick C disease. *Brain Pathol.* **8:** 163–174.
43. Chang, T. Y., P. C. Reid, S. Sugii, N. Ohgami, J. C. Cruz, and C. C. Y. Chang. 2005. Niemann-Pick type C disease and intracellular cholesterol trafficking. *J. Biol. Chem.* **280:** 20917–20920.
44. Vanier, M. T., and G. Millat. 2003. Niemann-Pick disease type C. *Clin. Genet.* **64:** 269–281.
45. Li, H., J. J. Repa, M. A. Valasek, E. P. Beltroy, S. D. Turley, D. C. German, and J. M. Dietschy. 2005. Molecular, anatomical, and biochemical events associated with neurodegeneration in mice with Niemann-Pick type C disease. *J. Neuropathol. Exp. Neurol.* **64:** 323–333.
46. Suzuki, M., Y. Sugimoto, Y. Ohsaki, M. Ueno, S. Kato, Y. Kitamura, H. Hosokawa, J. P. Davies, Y. A. Ioannou, M. T. Vanier, et al. 2007. Endosomal accumulation of Toll-like receptor 4 causes constitutive secretion of cytokines and activation of signal transducers and activators of transcription in Niemann-Pick disease type C (NPC) fibroblasts: a potential basis for glial cell activation in the NPC brain. *J. Neurosci.* **27:** 1879–1891.
47. Brown, M. S., and J. L. Goldstein. 1979. Receptor-mediated endocytosis: insights from the lipoprotein receptor system. *Proc. Natl. Acad. Sci. USA.* **76:** 3330–3337.
48. Innerarity, T. L., and R. W. Mahley. 1978. Enhanced binding by cultured human fibroblasts of apo-E-containing lipoproteins as compared with low density lipoproteins. *Biochemistry.* **17:** 1440–1447.
49. Herz, J., and H. H. Bock. 2002. Lipoprotein receptors in the nervous system. *Annu. Rev. Biochem.* **71:** 405–434.
50. Turley, S. D., D. K. Burns, C. R. Rosenfeld, and J. M. Dietschy. 1996. Brain does not utilize low density lipoprotein-cholesterol during fetal and neonatal development in the sheep. *J. Lipid Res.* **37:** 1953–1961.
51. Beffert, U., P. C. Stolt, and J. Herz. 2004. Functions of lipoprotein receptors in neurons. *J. Lipid Res.* **45:** 403–409.
52. Mauch, D. H., K. Nägler, S. Schumacher, C. Göritz, E-C. Müller, A. Otto, and F. W. Pfrieger. 2001. CNS synaptogenesis promoted by glia-derived cholesterol. *Science.* **294:** 1354–1357.
53. Pfrieger, F. W. 2003. Outsourcing in the brain: do neurons depend on cholesterol delivery by astrocytes? *Bioessays.* **25:** 72–78.
54. German, D. C., E. M. Quintero, C-L. Liang, B. Ng, S. Punia, C. Xie, and J. M. Dietschy. 2001. Selective neurodegeneration, without neurofibrillary tangles, in a mouse model of Niemann-Pick C disease. *J. Comp. Neurol.* **433:** 415–425.
55. German, D. C., C-L. Liang, T. Song, U. Yazdani, C. Xie, and J. M. Dietschy. 2002. Neurodegeneration in the Niemann-Pick C mouse: glial involvement. *Neuroscience.* **109:** 437–450.
56. Pentchev, P. G., M. T. Vanier, K. Suzuki, and M. C. Patterson. 1995. Niemann-Pick disease type C: a cellular cholesterol lipidosis. *In* The Metabolic and Molecular Bases of Inherited Diseases. C. R. Scriver, A. L. Beaudet, W. S. Sly, D. Valle, J. B. Stanbury, J. B. Wyngaarden, and D. S. Fredrickson, editors. McGraw-Hill, New York. 2625–2639.
57. Sokol, J., E. J. Blanchette-Mackie, H. S. Kruth, N. K. Dwyer, L. M. Amende, J. D. Butler, E. Robinson, S. Patel, R. O. Brady, M. E. Comly, et al. 1988. Type C Niemann-Pick disease. Lysosomal accumulation and defective intracellular mobilization of low density lipoprotein cholesterol. *J. Biol. Chem.* **263:** 3411–3417.
58. Blanchette-Mackie, E. J., N. K. Dwyer, L. M. Amende, H. S. Kruth, J. D. Butler, J. Sokol, M. E. Comly, M. T. Vanier, J. T. August, R. O. Brady, et al. 1988. Type-C Niemann-Pick disease: low density lipoprotein uptake is associated with premature cholesterol accumulation in the Golgi complex and excessive cholesterol storage in lysosomes. *Proc. Natl. Acad. Sci. USA.* **85:** 8022–8026.